Indian Journal of Pure & Applied Physics
Vol. 56, December 2018, pp. 970-977

Synthesis, characterization and electrical properties of GO/PANI/NPs (NPs = CdSe, CdSe/CdS, CdSe/ZnS) nanocomposites

D K Gupta[a,b]*, M Verma[b], R Gopal[c], N D Jasuja[a], K B Sharma[b] & N S Saxena[b]

[a]Faculty of Basic and Applied Sciences, Vivekananda Global University, Jaipur 303 012, India
[b]SPSL, Department of Physics, University of Rajasthan, Jaipur 302 004, India
[c]Department of Chemistry, University of Rajasthan, Jaipur 302 004, India

Received 9 November 2017; accepted 15 May 2018

In this paper, GO/PANI/NPs (NPs = CdSe, CdSe/CdS, CdSe/ZnS) nanocomposites have been prepared using chemical method. The electrical properties of CdSe quantum dots, core shell nanoparticles (CdSe@CdS and CdSe@ZnS), graphene oxide/polyaniline nanocomposite (GO/PANI) and graphene oxide/polyaniline/nanoparticles (GO/PANI/NPs) nanocomposites have been measured using electrometer/high resistance meter (Keithley 6517A) at different wt% ratio. The above obtained nanoparticles (CdSe, CdSe@CdS and CdSe@ZnS) show the electrical current in nano ampere (nA) range while GO/PANI nanocomposites show the electrical current in miliampere (mA) range in the *I-V* measurement. The results of this study have been expected to reveal the effect of finite particle size on the conductivity of nanoparticles. The observed electrical conductivity of GO/PANI/NPs nanocomposites has been significantly reduced after the mixing of above obtained nanoparticles in different wt% ratio with GO/PANI nanocomposites. The knowledge of electrical conductivity and the effective mechanism for the conduction in nanocomposite is important for the fabrication of an electronic device such as solar cell.

Keywords: Graphene oxide/polyaniline/NPs nanocomposite, Transmission electron microscopy, Electrometer/high, Resistance meter (Keithley 6517A).

1 Introduction

In the past few years, after discovery in 2004, graphene has attracted more attentions and been widely studied by the researchers[1]. Graphene is a carbon-based nanomaterial with single-atom thickness and due to the unique structure and remarkable mechanical, optical, thermal and electrical properties, graphene has been studied to produce high-performance polymer composites[2,3]. Graphene oxide (GO) is a chemically modified graphene sheet, which contains a wide range of oxygen functional groups such as epoxide, alcohol, and carboxylic acid both on the basal planes and at the edges of the sheets[4]. GO could be easily modified to produce homogeneous colloidal suspensions to synthesize the graphene-based materials due to existence of these oxygen functional groups[5]. Now a days, GO has been widely used in nanoelectronics[6], electrochemical sensors and biosensors[7,8], lithium battery[9], and supercapacitor[10], etc. The different GO-based nanocomposites have also been synthesized and used to construct the biosensor. The GO based composites using polystyrene[11], polyaniline[12], Au nanoparticles[13], etc., were synthesized to entrap enzymes and proteins for biosensing.

The dispersion of graphene within different polymer matrices has made the new class of polymer nanocomposites[14]. The development of nanocomposite materials speaks to a productive route to enhance the exhibitions of polymer and extend their application scopes.

Advantages of graphene oxide (GO) are easy dispersibility in water and other organic solvents due to the presence of oxygen and hydroxyl functionalities[15]. This remains a very important property when mixing with polymer matrices to improve their spectroscopic, electrical and mechanical properties. GO can be obtained by the exfoliation of graphite yielding well separated two-dimensional[16]. It offers extraordinary electronic, thermal and mechanical properties. Many reports have been made not only on graphene's very high electrical conductivity at room temperature but also its potential use as nano-sensors, transparent electrodes and many other applications[17].

GO/PANI nanocomposites have excellent optical, electrical, and other physical and chemical properties. GO/PANI nanocomposites have been widely studied in the area of nanoelectronic devices, sensors, energy

*Corresponding author
(E-mail: deepak.nanoconverge@gmail.com)

storage and conversion, bioscience and technology[18]. Polyaniline (PANI) is a polymer and widely used due to its relatively easy preparation and high degree of electric conductivity[19,20].

During the last two decades, group II -VI semiconductor nanoparticles have been of great current interest due to their novel physical and chemical properties[21,22]. Three-dimensional confinement of charge carriers in quantum dots (QDs) transforms continuous optical spectra of a bulk semiconductor into discrete atomic-like spectra. Quantum confinement of charge carriers alters many properties of nano particles including electrical conductivity. These variations in electrical properties are the results of band structure modification, the predominant contribution of the largely defective and strained grain boundaries in nano materials[23-25].

In polycrystalline semiconductors, the electrical properties are often predominated by a double depletion layer that forms around grain boundaries[26,27]. According to grain-boundary trapping theory, free carriers are trapped by the trapping states at the boundary causing a depletion of free charges in the grain region nearest to the boundary[28]. That depletion causes space charges which establish an energy barrier between two adjacent grains. This grain boundary potential barrier extends over a length corresponding to the Debye screening length[29]. When the grain size becomes comparable to the Debye screening length electrons are trapped at the interface or in the surface states and the grain interior becomes entirely depleted of electrons.

In small size nanocrystalline materials, the carriers are effectively captured in the traps at grain boundaries. However, in larger samples, the number of traps per volume may be smaller, and hence number of electrons trapped at the interface will also be smaller. It was also reported in the case of semiconductors that, when grain size decreases, there is a greater chance for charge carriers to escape to the surface[30]. Quantum mechanical tunneling and barrier emission are two distinct mechanisms whereby an electron or a hole incident to a potential barrier can reach the other side[31]. As the size of QDs decreases the possibility of more charge carriers being trapped in shallow trap states for smaller size QDs increases.

In the present paper, synthesis, characterization and electrical properties of GO/PANI/NPs nanocomposites have been studied. The results of this study are expected to reflect the effect of finite grain size on the conductivity of nanocomposite. For electrical measurement, the nanocomposite samples were prepared in the form of cylindrical compacts having a diameter of 10mm and a thickness of about 1mm by applying a uniaxial pressure of 100kg/cm^2 for 1 min using a hydraulic press. All the samples were prepared under the same conditions. The conductivity of all the samples has been determined through the I-V measurements using the electrometer at room temperature.

2 Experimental Method

2.1 Materials

Materials used were graphite flakes, sodium nitrite, hydrogen peroxide (30%), sulphuric acid (70%), and potassium permanganate (99%), aniline, ammonium per sulfate, dihydrate purified ($(CH_3COO)_2Cd.2H_2O$, ≥98%, Merck), highly pure Selenium powder (Se, 99.99% HPLC), trioctyl phosphene oxide (TOPO, 99%, Aldrich), trioctyl phosphene (TOP, 97%, Aldrich), hexadecyl amine (HDA, 98%, Aldrich), tetradecyl phosphonic acid (TDPA, 97%, Aldrich) etc.

2.2 Preparation of GO/PANI/NPs nanocomposite

In a typical recipe, graphene oxide (GO) was prepared from graphite powder by a modified Hummers method according to the literature[32-34]. The GO was dispersed in aqueous solution (100 mg/ 30 mL) by ultra-sonication. 2 mL of aniline in 0.5M HCl were introduced in aqueous solution of GO. The dispersed solution was ultrasonicated for another 25 min. Then 1.5 mg of ammonium per sulfate dissolved in 0.5M HCl was added drop wise into the reaction system and stirred continuously for 2 h. The precipitates were collected by filtration and repeatedly washed with deionized water, ethanol, and dried at 50°C in vacuum for 24 h[35,36].

CdSe quantum dots and core shell nanoparticles (CdSe@CdS, CdSe@ZnS) were prepared using the procedure mentioned in the literature[37,38]. To prepare GO/PANI/NPs nanocomposites, 0.5 mg/mL GO/PANI solution was mixed with NPs solution with the volume ratio of 1:3 by mild sonication for 10 min. The precipitates were collected by centrifugation and repeatedly washed with deionized water, ethanol, and dried it at 50°C in vacuum for 24 h[39,40].

2.3 Characterization techniques

The above synthesized GO/PANI/NPs nanocom posites were characterized for their crystal structure and phase using Panalytical Xpert Pro X-ray Diffractometer (XRD) operating at 40 kV and 35mA

with λ = Cu-Kα (1.5418 Å) radiation in an angle range of 100 to 700. Transmission electron microscopy (TEM) investigations were carried out using Tecnai 20 G2 S-Twin TEM with e-beam voltage of 200 kV. Chemical bonding was determined by using Fourier transform infrared spectroscopy (IR Affinity, Shimadzu). Electrical properties have been measured using Electrometer/ High Resistance Meter (Keithley 6517A).

3 Results and Discussion

3.1 Structural and morphological characterization of GO/PANI/NPs nanocomposites

Figures 1 and 2 show the X-ray diffractograms of GO/PANI and GO/PANI/NPs nanocomposite. The peaks centered at 2θ values of 15.3°, 20.54° and 25.26°, correspond to (011), (020) and (200) planes which are the characteristic Bragg diffractions of PANI[41,42]. We observed that for GO/PANI there is a weak peak with low intensity which appears at 2θ=11.38° which is due to graphene oxide. No impurity-related ripples or small peaks were observed in all spectra, demonstrating the purity and good dispersion of GO in PANI polymeric matrices. The increase in the broadness of this peak reveals the increase of these amorphous regions in the samples. The interaction between the PANI and GO results in decreasing crystallinity with rich amorphous phase. The amorphous nature is responsible for higher conductivity and affirms the complexation between GO and PANI[43]. XRD pattern of GO/PANI/NPs is more or less similar to that of the XRD of PANI/NPs and the absence of GO reflection peak in GO/PANI/NPs confirms that GO is covered by PANI[39]. In the XRD pattern of GO/PANI/CdSe nanocomposite, diffraction

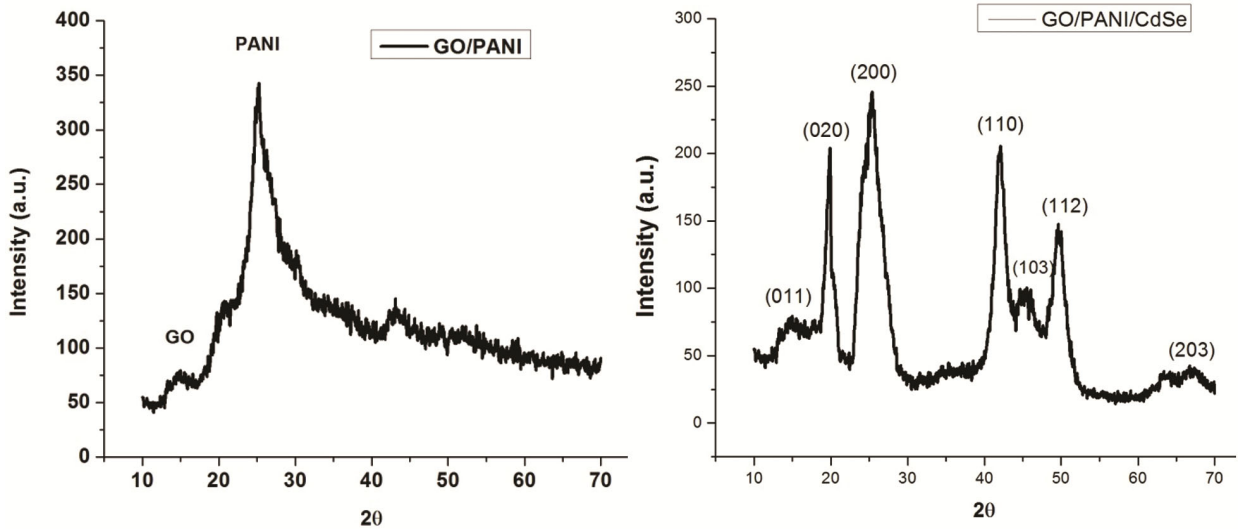

Fig. 1 — XRD pattern of GO/PANI and GO/PANI/CdSe nanocomposites.

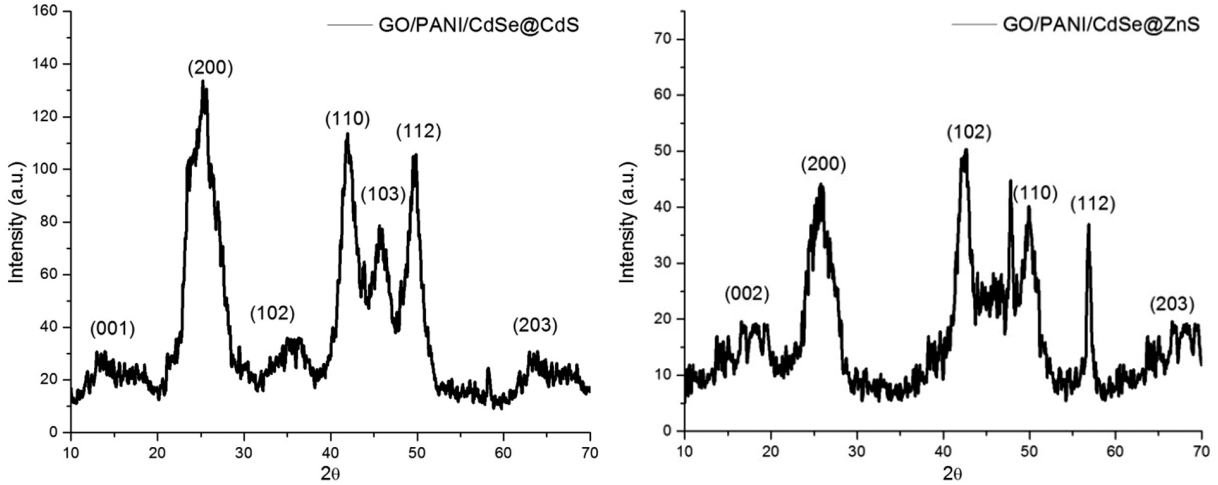

Fig. 2 — XRD pattern of GO/PANI/CdSe@CdS and GO/PANI/CdSe@ZnS nanocomposites.

peaks at angles (2θ) 25.391, 41.9990, 45.8100, 49.7180, 63.8840 which correspond to planes (002), (110), (103), (112), (203) of CdSe are present along with GO/PANI peak. In the XRD pattern of GO/PANI/CdSe@CdS and GO/PANI/CdSe@ZnS nanocomposite (Fig. 2), diffraction peak of core/shell (CdSe@CdS and CdSe@ZnS) is present along with PANI peak.

The TEM image of GO/PANI/NPs (NPs = CdSe, CdSe@CdS and CdSe@ZnS) nanocomposite is shown in Fig. 3. As shown from Fig. 3, some corrugations of GO sheet, nano structure of PANI and (a) CdSe quantum dots or (b-c) core/shell nanoparticles (CdSe@CdS and CdSe@ZnS) nanoparticles were clearly observed in our sample. The growth of PANI on the graphene surface is difficult to observe by TEM images due to the much smaller size of the graphene nanosheets.

The EDAX measurements of the synthesized GO/PANI/CdSe nanocomposite were performed using a Tecnai 20 G^2 S-Twin TEM fitted with an EDAX (Bruker Company). EDAX of sample has been shown in Fig. 4. EDAX of sample in Table 1 shows

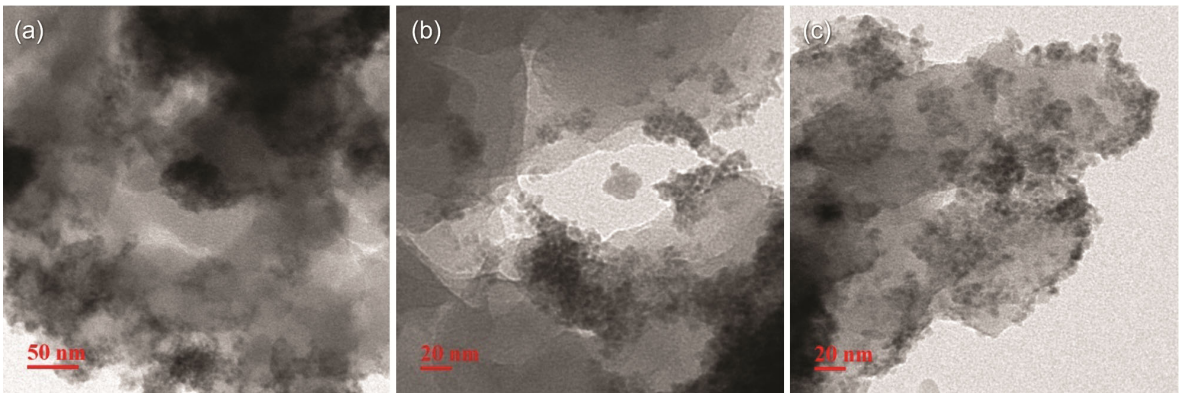

Fig. 3 — TEM micrograph of (a) GO/PANI/CdSe, (b) GO/PANI/CdSe@CdS and (c) GO/PANI/CdSe@ZnS nanocomposites.

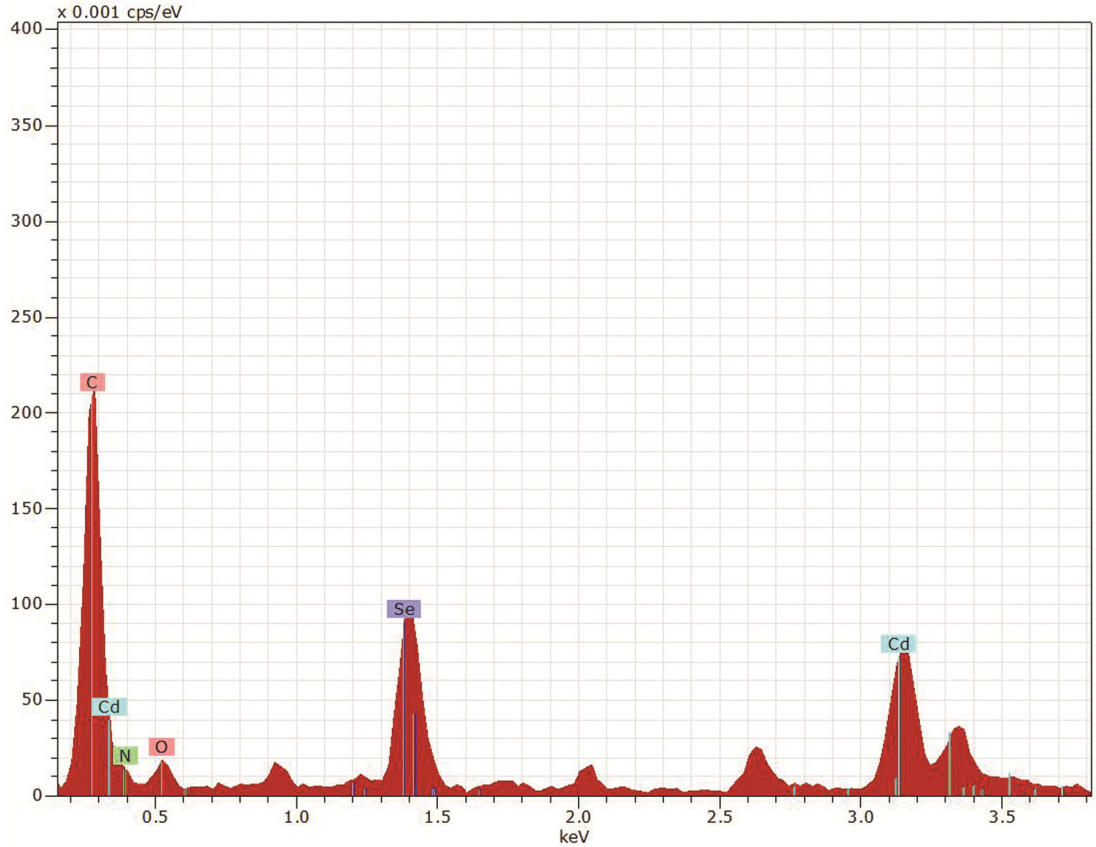

Fig. 4 — EDX micrographs of GO/PANI/CdSe nanocomposite.

graphene, PANI, cadmium and selenium present in the sample to be in a stoichiometric atomic ratio.

The additional evidence in the synthesis of GO/PANI and GO/PANI/NPs nano composites is provided by the Fourier transforms infrared (FT-IR) spectra shown in the Figs 5 and 6. In Fig. 5 (a), the typical FT-IR of graphene oxide peaks located at 1496 cm^{-1} are showing the stretching and bending of the widespread O–H groups in the sample. The characteristic peaks of oxygen are located at wave number of 1164 cm^{-1} which are corresponding to C–O (epoxy or alkoxy) bond. This suggests that the oxidation of graphite took place during synthesis using modified Hummers method which is consistent with the existing literature. The PANI shows C=C stretching vibration band at 1498 cm^{-1}, is attributable to the benzenoid which is overlapped with graphene oxide peaks located at 1496 cm^{-1} . In addition, a stretching band[44,45] assigned to C–N also appears at 1300 cm^{-1}. The FT-IR spectrum of GO/PANI/NPs in Fig. 5 (b) and Fig. 6 (a,b) show peaks of both GO, PANI and CdSe or core shell (CdSe@CdS and CdSe@ZnS) functional groups. Figure 6 shows some chief characteristic bands of polyaniline observed in the GO/PANI/NPs nanocomposite. Such as, the bands at 3133, cm^{-1} is attributed to N-H stretching in the quinoid ring of the emeraldine base and emeraldine salt,

Table 1 — Elemental analysis of GO/PANI/CdSe nanocomposite

EL	AN	Series	Unn. C [wt. %]	Norm. C [wt. %]	Atom. [wt. %]	C Error (1 Sigma) [wt. %]
C	6	K-series	79.82	79.82	96.14	2.81
Cd	48	L-Series	12.26	12.26	1.58	1.28
Se	34	K-series	6.86	6.86	1.26	0.31
N	7	K-series	0.55	0.55	0.57	0.09
O	8	K-series	0.51	0.51	0.46	0.07
		Total	100	100	100	

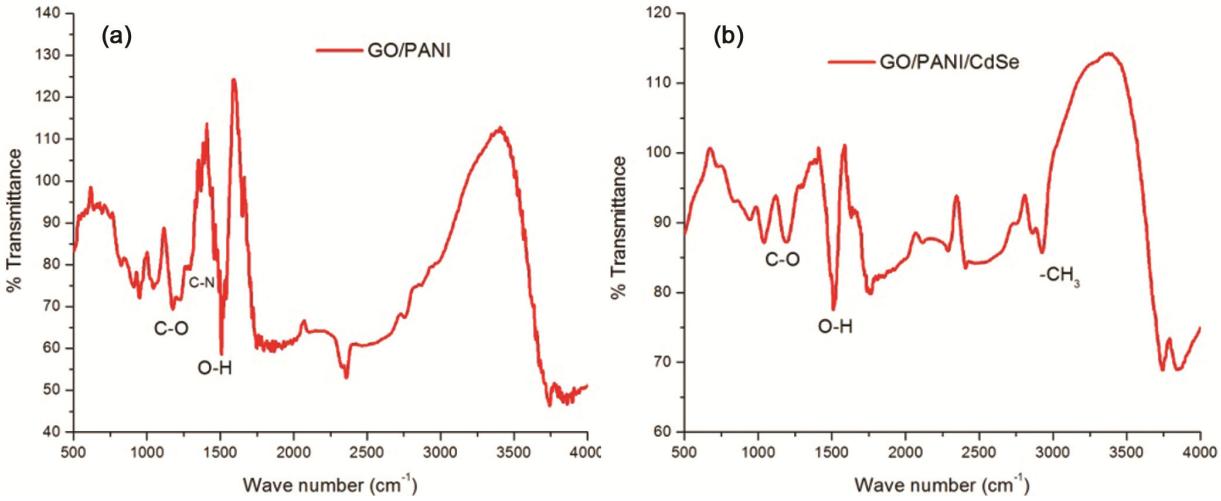

Fig. 5 — FTIR spectra of (a) GO/PANI and (b) GO/PANI/CdSe nanocomposites.

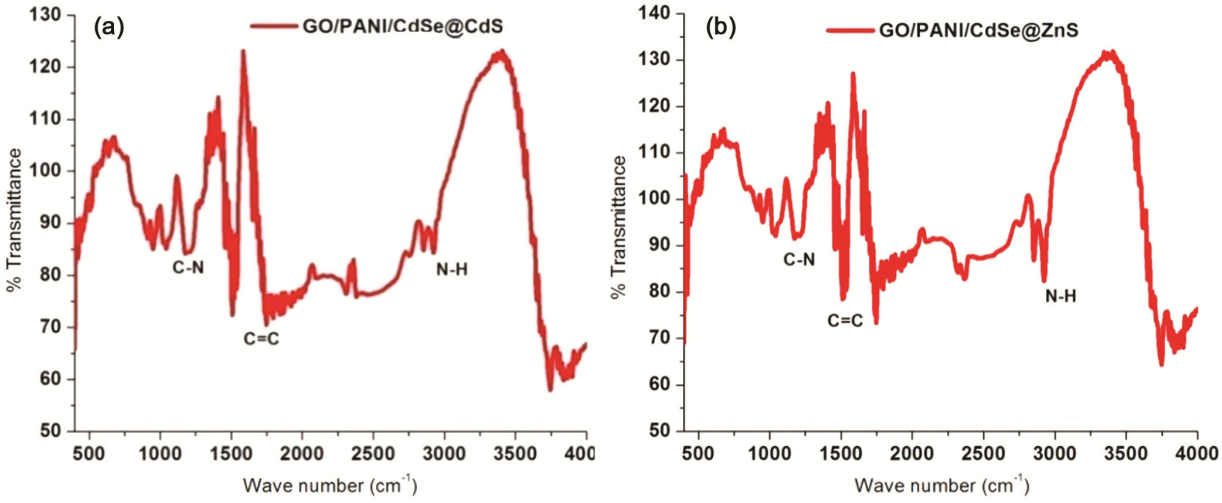

Fig. 6 — FTIR spectra of (a) GO/PANI/CdSe@CdS and (b) GO/PANI/CdSe@ZnS nanocomposites.

1604 cm^{-1} is attributed to C=C stretching in the quinoid ring of the emeraldine base and emeraldine salt and 1303 cm^{-1} is attributed to C-N stretching, respectively. These results illustrate that this resulting-product contained polyaniline.

3.2 Electrical studies of GO/PANI/NPs nanocomposites

CdSe quantum dots and core shell (CdSe@CdS and CdSe@ZnS) nanoparticles show the electrical current in nano ampere (nA) range (Fig. 7). The observed dc electrical current of above obtained nanoparticles of small grain size and large grain boundaries can be explained within the framework of electrical transport in polycrystalline semiconductors that have potential barriers at grain boundaries.

Electrical conductivity of GO/PANI and GO/PANI/CdSe has been shown in Fig. 8. Current-voltage characteristics of GO/PANI/CdSe@CdS and GO/PANI/CdSe@ZnS nanocomposites have been shown in Fig. 9. When we mix the above obtained

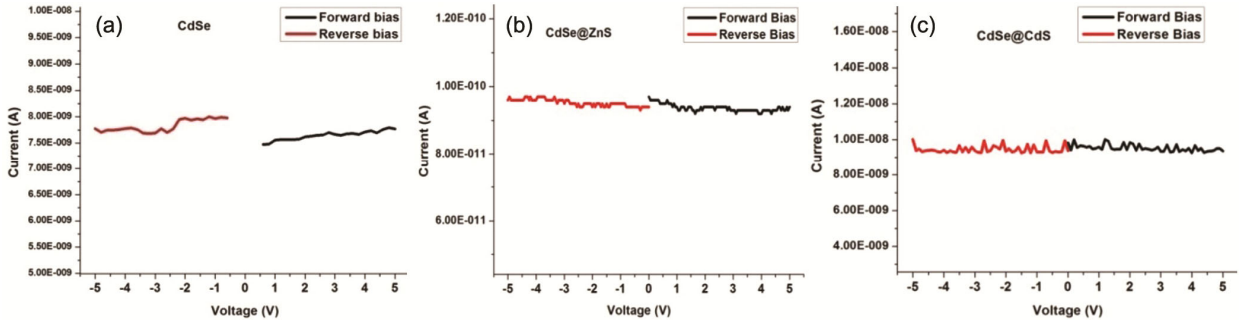

Fig. 7 — *I-V* curves of (a) CdSe, (b) CdSe@CdS and (c) CdSe@ZnS nanoparticles.

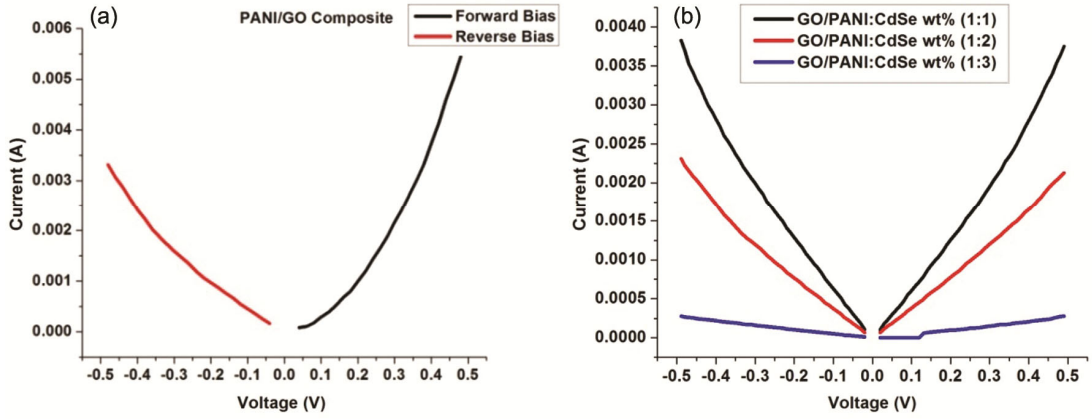

Fig. 8 — *I-V* curves of (a) GO/PANI and (b) GO/PANI/CdSe nanocomposite at different wt% ratio.

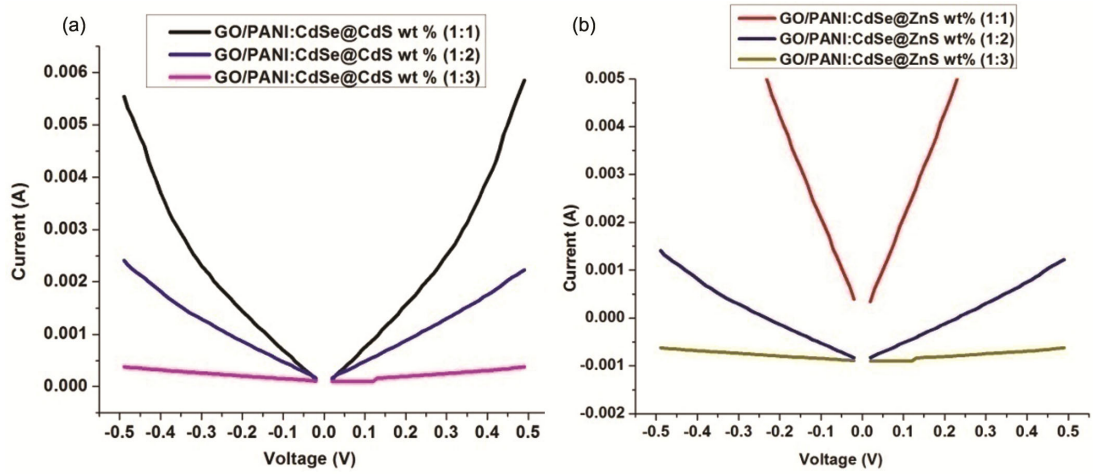

Fig. 9 — *I-V* curves of (a) GO/PANI/CdSe@CdS and (b) GO/PANI/CdSe@ZnS nanocomposite at different wt% ratio.

nanoparticles in different wt% ratio with GO/PANI nanocomposites, the electrical behavior of nanocomposite is significantly changed according to different wt% ratio of nanoparticles (CdSe or CdSe@CdS or CdSe@ZnS). When we mix the GO/PANI with described nanoparticles in 1:1 wt % ratio, the electrical current of GO/PANI/NPs nanocomposite is almost similar to GO/PANI nanocomposite. This may be due to the dominating electrical conduction of GO/PANI as compared to NPs for 1:1 wt % ratio. When we mix the GO/PANI with NPs in 1:2 wt % ratio, the electrical conductivity of composite lies between the electrical conductivity of GO/PANI and NPs. Finally when we mix the GO/PANI and NPs in 1:3 wt % ratio, the electrical conductivity of composite is similar to NPs conductivity.

4 Conclusions

The GO/PANI/NPs nano composite were effectively synthesized and structurally characterized by XRD, TEM, EDX and FTIR. NPs and GO/PANI nanocomposites show the electrical current in nano ampere (nA) and miliampere (mA) range, respectively. The electrical behavior of GO/PANI/NPs nanocomposites is significantly reduced according to different wt% ratio of NPs which might be due to dominating electric conduction in GO/PANI over the electrical conduction in NPs. The GO/PANI nanocomposites would have potential applications in chemical sensors, biosensors or flexible nanoelectronic devices in the light of their electrical conduction.

Acknowledgment

One of the authors Professor N S Saxena gratefully acknowledge UGC, New Delhi (India) for providing financial support in the form of Emeritus fellowship.

References

1 Novoselov K S, Geim A K, Morozov S V, Jiang D, Zhang Y, Dubonos S V, Grigorieva I V & Firsov A A, *Science*, 306 (2004) 666.
2 Stampfer C, Schurtenberger E, Molitor F, Guttinger J, Thn T & Ensslin K, *Nano Lett*, 8 (2008) 2378.
3 Li D & Kaner R B, *Science*, 320 (2008) 1170.
4 Cai W, Piner R D, Stadermann F J, Park S, Shaiba M A, Ishii Y, Yang D, Velamakanni A, An S J, Stoller M, An J, Chen D & Ruoff R S, *Science*, 321 (2008) 1815.
5 Park S J, An J, Jung I, Piner R D, An S J, Li X, Velamakanni A & Ruoff R S, *Nano Lett*, 9 (2009) 1593.
6 Savchenko A, *Science*, 323 (2009) 589.
7 Liu Y X, Dong X C & Chen P, *Chem Soc Rev*, 41 (2012) 2283.
8 Wang Y, Li Y M, Tang L H, Lu J & Li J H, *Electrochem Commun*, 1 (2009) 889.
9 Wang C Y, Li D, Too C O & Wallace G G, *Chem Mater*, 21 (2009) 2604.
10 Zhang S L, Li Y M & Pan N, *J Power Sources*, 206 (2012) 476.
11 Hu H T, Wang X B, Wang J C, Wan L, Liu F M, Zheng H, Chen R & Xu C H, *Chem Phys Lett*, 484 (2010) 247.
12 Sheng K X, Bai H, Sun Y Q, Li C & Shi G Q, *Polymer*, 52 (2011) 5567.
13 Gute A, Carraro C & Maboudian R, *Biosens Bioelectron*, 33 (2012) 56.
14 Wang J, Tong X & Zhang Y, *Asian J Chem*, 23 (2011) 2281.
15 Zhu Y, Murali S & Cai W, *Adv Mater*, 22 (2010) 3906.
16 Marcano D C D, Kosynkin D D V, Berlin J M, et al, *ACS Nano*, 4 (2010) 4806.
17 Gómez-Navarro C, Weitz R T, Bittner A M, Scolari Matteo, Mews Alf, Burghard Marko & Kern Klaus, *Nano Lett*, 7 (2007) 3499.
18 Zheng J, Ma X, He X, Gao M & Li G, *Proc Eng*, 27 (2012) 1478.
19 Pan L J, Pu L, Shi Y, Sun T, Zhang R & Zhang Y D, *Adv Funct Mater*, 16 (2006) 1279.
20 Gangopadhyay R & De A, *Chem Mater*, 12 (2000) 608.
21 Gupta D K, Verma M, Patidar D, Sharma K B & Saxena N S, *Adv Sci Lett*, 22 (2016) 3893.
22 Gupta D K, Verma M, Patidar D, Sharma K B & Saxena N S, *Adv Sci Lett*, 22 (2016) 3897.
23 Dwivedi D K, Dayashankar & Dubey M, *J Ovonic Res*, 5 (2009) 35.
24 Tsujimoto Y, Matsushita Y, Yu S, Yamaura K & Uchikoshi T, *J Asian Ceram Soc*, 3 (2015) 325.
25 Suresh S & Arunseshan C, *Appl Nanosci*, 4 (2014) 179.
26 Pike G E & Seager C H, *J Appl Phys*, 50 (1979) 3414.
27 Seager C H & Pike G E, *Appl Phys Lett*, 35 (1979) 709.
28 Seto J Y W, *J Appl Phys*, 46 (1975) 5247.
29 Nan C W, Schope T, Holten S, Kleim H & Birringer R, *J Appl Phys*, 85 (1999) 7735.
30 Slender J A, *Chem Rev*, 87 (1987) 877.
31 Seager C H & Castner T G, *J Appl Phys*, 49 (1978) 3879.
32 Hummers W S & Offerman R E, *J Am Chem Soc*, 80 (1958)1339.
33 Kovtyukhova N I, Ollivier P J, Martin B R, Mallouk T E, Chizhik S A, Buzaneva E V & Gorchinskiy A D, *Chem Mater*, 11 (1999) 771.
34 Gupta D K, Rajaura R S & Sharma K B, *Sci Technol*, 1 (2015)16.
35 Xu G, Wnag N, Wei J, Lv L, Zhang J, Chen Z & Xu Q, *Ind Eng Chem Res*, 51 (2012) 14390.
36 Rajaura R S, Sharma V, Ronin R S, Gupta D K, Srivastava S, Agrawal K & Vijay Y K, *Mater Res Exp*, 4 (2017) 2.
37 Gupta D K, Verma M, Sharma K B & Saxena N S, *Indian J Pure Appl Phys*, 55 (2017) 113.
38 Gupta D K, Verma M, Patidar D, Sharma K B & Saxena N S, *Nanosci Nanotechnol Asia*, 7 (2017) 73.
39 Hu X W, Mao C J, Song J M, Niu H L, Zhang S Y & Huang H, *Biosens Bioelectron*, 41 (2013) 372.
40 Gupta D K, Verma M, Kumari V, Sharma K B & Saxena N S, *Technol Lett*, 4 (2017) 5.
41 Wang H, Hao Q, Yang X, Lu L & Wang X, *Electrochem Commun*, 11 (2009) 1158.
42 Xu J, Wang K, Zu S, Han B & Wei Z, *ACS Nano*, 4 (2010) 5019.

43 Elashmawiab N I S, Alatawic N S & Elsayedd H, Res Phys, 7 (2017) 636.

44 Azizah N, Hashim U, Arshad M K, Gopinath S C B, Nadzirah S, Farehanim M A, Fatin M F, Muaz A K M, Ruslinda A R & Ayub R M, *ARPN J Eng Appl Sci*, 11 (2016) 8889.

45 Lu L, Xu X L, Liang W T & Lu H F, *J Phys Condens Matter*, 19 (2007) 406221.